3. Excitation and Detection of Fluorescence

In this chapter, we examine key experimental components and methods to observe weakly fluorescing objects. We consider in turn the excitation source, the detectors, the spectrally selecting elements which will reject the excitation light (much more intense than the fluorescence), and the ways to analyse the stream of fluorescence photons.

3.1. Light sources

The only light sources used in practice are lasers, for their high spatial mode quality, for their intensity, and for their spectral purity. Note, however, that most lasers also present residual fluorescence emission around the laser line (plasma lines for gas lasers, broad bands for dye, solid-state or semiconductor lasers). To detect the weak fluorescence emission from single molecules, it is exceedingly important to eliminate this residual light from the excitation beam. Narrow band-pass interference filters (laser-line filters, or 'clean-up' filters) are often sufficient for that purpose. Depending on the experiments, two main types of lasers are used :

3.1.1 continuous-wave (cw) lasers: In gas lasers (He-Ne, Ar^+, Kr^+), the emitting species are ions or atoms in a gas or plasma. These sources deliver high power (up to 20 W for argon ion lasers) on fixed narrow lines. Usual lasers can be operated on several different lines, or on all lines at once. Dye lasers use fluorescing molecules in solutions. Certain solid-state lasers (Ti-sapphire 700-1000 nm, Cr-forsterite 1150-1350 nm), and semiconductor lasers (diode lasers) present broad bands or broad lines. All these broad-band lasers are tunable by placing selective elements in the laser cavity. This is a big advantage for spectroscopy. Other solid-state lasers (Nd-YAG, diode-pumped solid state lasers, fiber lasers) work at fixed wavelengths and are not tunable). Nowadays, frequency-doubled Nd-YAG lasers at 532 nm are the most usual pump lasers for Ti-Sapphire and dye lasers.

Cw-lasers can be frequency-stabilized passively or actively on stable frequency references, making high-resolution spectroscopy possible. They are widely used in atomic physics, and in the spectroscopy of solids at low temperatures, notably single-molecule spectroscopy at cryogenic temperatures (cf. Chapters 8-13).

3.1.2 pulsed lasers: Pulsed operation may follow from pulsed excitation (either through electric discharges as in nitrogen lasers, or from pulsed optical pumping with

flash lamps as in powerful Nd-YAG lasers). More often nowadays, pulses are obtained via mode-locking a cw laser with broad gain band. A very common source is a Ti-sapphire laser providing pulses between 100 fs and 10 ps at a high repetition rate of 80 MHz (determined by the cavity length). Electric pumping of diode lasers can also be pulsed at about 100 MHz with pulse durations of some tens of ps, leading to convenient sources for fluorescence microscopy and lifetime imaging. Pulsed lasers are used in fluorescence lifetime measurements and in the generation of new wavelengths and of various useful nonlinear optical effects thanks to their high peak intensities. Generation of new wavelengths proceeds via nonlinear optics by frequency doubling (second-harmonic generation SHG) or mixing (sum frequency generation SFG), parametric generation (optical parametric oscillator OPO, or amplifier OPA), and also for nonlinear laser spectroscopy such as coherent Raman scattering. Because most nonlinear effects depend quadratically or with higher powers on laser intensity along the optical axis, their generation profile is much steeper than that of linear effects such as fluorescence. Therefore, nonlinear optics often present the property of *optical sectioning* of a 3-dimensional sample, introduced in Ch. 2 about confocal microscopy. Optical sectioning by a nonlinear effect such as SHG or two-photon excited fluorescence gives the signal of the slice of sample where the excitation beams are focussed without a pinhole, because other slices in front or at the back of the focus do not generate any significant background.

3.2. Detectors

The fluorescence signal of a single molecule is rather weak, often much lower than 1 Mcps (million counts per second), sometimes as low as 10 cps. Therefore, it is important to reduce noise and background sources as much as possible. The best way to reduce electronic background in weak optical signals is to count photons individually, with photon-counting detectors. The threshold used to discriminate the photon signal from background is a very efficient nonlinear noise filter. However, optical background from stray light and from detector dark counts of course remains. For a perfectly constant incoming intensity, a photon-counting detector's signal is *shot-noise-limited*. Fluctuations only arise from the statistics of random but independent detection events, at least for count rates much lower than the detector's saturation rate. Photon noise (or shot noise) is the lowest noise limit for "natural"

light. Quantum-optical methods make it possible to prepare “squeezed” states of light in which fluctuations are reduced compared to those of natural light.

3.2.1. Photomultiplier tube (PMT): in the photoelectric effect, a photon rips an electron off a sensitive material in a vacuum tube. This electron is accelerated, “amplified” by hitting dynodes. After several (5-10) dynodes, the amplification factor is of the order of one million, leading to a measurable charge pulse. This pulse is detected and shaped by a low-noise preamplifier. A discriminator rejects all pulses and fluctuations with charge less than a pre-set threshold. The main detector features are:
- its spectral response, which depends on the photocathode (typical GaAs 400-900 nm, S20 bialkali 300-600 nm, some cathodes are sensitive until 1700 nm).
- its quantum yield; the detection yield of a good PMT can reach 20-30%, but more often is 10% or less.
- its dark count rate; this rate is typically less than 50 cps and can be lower than a few cps in some cases.
- its maximum count rate, which determines the time resolution. Photon-counting PMT’s are usually limited to 1 Mcps at best.
- its sensitive area; this area is of the order of several tens of mm^2 for PMT’s, although it can reach several cm^2 in some cases. The large sensitive area makes optical adjustments easy, and require only very simple optics. Such a large area is useless to detect light from microscopes, which provide diffraction-limited optics and can be easily focused to 100 μm or less. Therefore, in fluorescence microscopy, PMT’s have been replaced by avalanche photodiodes.

3.2.2 Single-photon avalanche photodiode (APD): it is a solid-state version of the PMT. The discharge (avalanche) must be actively quenched to safeguard the component, and also to increase the maximum count rate (10 to 20 Mcps). Most APD’s are made of Si, with a spectral range 400-1100 nm (300-1100 nm if UV-enhanced). The quantum yield is very good, up to 70% around 700 nm. However, in order to limit the dark-count rate to typically 100 cps, or to less than 10 in the best individual cases, the sensitive area has to be limited to 125 μm in diameter. Therefore, an APD can only be used with very good optics, for example with microscope

objectives. It is the combination of high-quality microscope objectives and APD's that has made single-molecule detection at room temperature a standard technique.

3.2.3 Charge-coupled devices: a CCD camera is a 2D matrix of independent photodiode detectors. Each detector is coupled to a capacitor which stores photogenerated charge carriers during the accumulation time. Upon reading, the contents of each capacitor are transferred line by line, and the last line is read by a special register. The main advantage of the CCD is to be a multichannel detector, allowing one-step acquisition of a whole picture. Further, the dark count rate of CCD is very low. Typical rates are much less than 1 cps per pixel, which is ideal for low light levels, as e. g. in astronomy, and allows for very long recording times, limited mainly by cosmic rays and background radioactivity. The spectral response is in most cases that of Si. Other semiconductors are also available, albeit at a high price. The quantum yield reaches 80% at 700 nm for the back-thinned CCD's (the front-illuminated ones only reach 50 %). Their main drawback is the relatively slow acquisition: at least 1 ms is needed to read the whole matrix, more usual times are 10 ms or longer. The read-out step introduces additional noise. Intensified CCD cameras can be triggered for fast response, and they can count photons (whereas usual CCD's need about 4 photons to count one event), but their quantum yield is lower, typically comparable to that of a PMT. Recently, CCD's with on-chip amplification have become available. They combine the high quantum yield of Si with photon-counting capability.

3.3. Filters and selective elements

The most effective way to separate fluorescence is spectral filtering (because of the spectral selection discussed in the introduction). Different types of filters are based on absorbing materials, or on optical interference.

Absorbing materials: Organic dyes in gelatine can be used to make absorptive filters (e.g., for photography), but their durability is poor. Colored-glass filters are preferred in spectroscopy. The most important ones use absorbing semiconductor nano-particles. Glass annealing makes it possible to control the size of these particles, and therefore their spectrum, via quantum confinement effects.

Multidielectric filters : a multilayer with an alternation of low- and high-index layers, each layer having a quarter-wave thickness, behaves as a stop-gap material for plane

waves of a given frequency at normal incidence. The reason is the constructive interference of beams reflected by all interfaces. The spectral width of the stop gap increases with the index contrast between the two materials, while the steepness of its spectral edges increases with the number of layers. The stop-gap can be slightly shifted to the blue at oblique incidence according to the variation of the optical path difference :

$\Delta l = 2nd\cos r$, n the refractive index, d the thickness, r the refraction angle (see Fig. 3.1).

An important special case is the holographic *notch* filter. A sinusoidal refractive index grating is written in a photosensitive gelatine material by a standing wave, obtained via interference of two laser beams. The index contrast is rather low, but the number of layers can be very large, with a good spatial coherence over a large area of filter. Such filters are narrow enough to cut off a laser line within 10 nm, which is very useful in Raman spectroscopy, but also for single-molecule fluorescence detection.

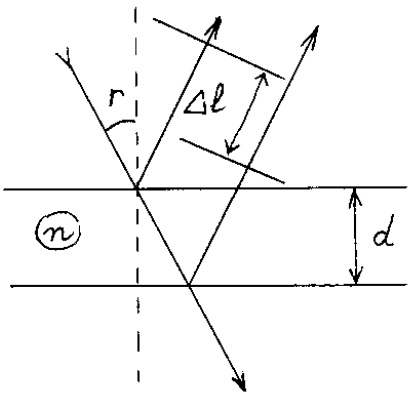

Figure 3.1: Optical path difference Δl between the reflections on the two faces of a layer with thickness d in a medium with refractive index n.

For more flexibility in central wavelength and width, one may use monochromators or acousto-optical tunable filters (AOTF's). These tunable narrow-band filters are based on diffraction by a grating or an acoustic standing wave, or on dispersion by a prism. The latter solution is nonlinear in wavelength, but has excellent throughput over a broad spectral range. By associating a monochromator and a CCD camera, one obtains a spectrograph, which can record a whole spectrum in one shot, and is not sensitive to intensity fluctuations of the source laser.

3.4. Photon-counting analysis

3.4.1. Cw light sources :

Even though the excitation rate may be constant, the photons emitted by a single nano-object can show distinct patterns in time. Hereafter, we discuss photon statistics in some important cases.

i) thermal or chaotic light:

Chaotic or thermal light arises from the superposition of the incoherent fields of many sources, so that the intensities of all these sources add up to yield the total intensity. Classically, this amounts to superimposing many fields from individual sources, with random phases:

$$\vec{E} = \sum_i e^{i\varphi_i} \vec{E}_0(t - t_i)$$

We have assumed that each source emits the same field at different times, with a different phase factor. One can define a first-order correlation function for this field, and this function is the same as that of one of the elementary sources:

$$g^{(1)}(\tau) = \frac{\langle E(t+\tau)E^*(t)\rangle}{\langle |E|^2(t)\rangle} = \frac{\langle E_0(t+\tau)E_0^*(t)\rangle}{\langle |E_0|^2(t)\rangle} \quad .$$

The field correlation function starts from 1 for short times and tends to 0 for long times. The emitted spectrum is obtained from the Wiener-Khinchin theorem relating it to the field correlation function by a Fourier transformation:

$$I(\omega) = |E(\omega)|^2 = \int e^{i\omega t} E(t)dt \int e^{-i\omega t'} E^*(t')dt' \quad \propto \quad FT\left(g^{(1)}(\tau)\right) \quad .$$

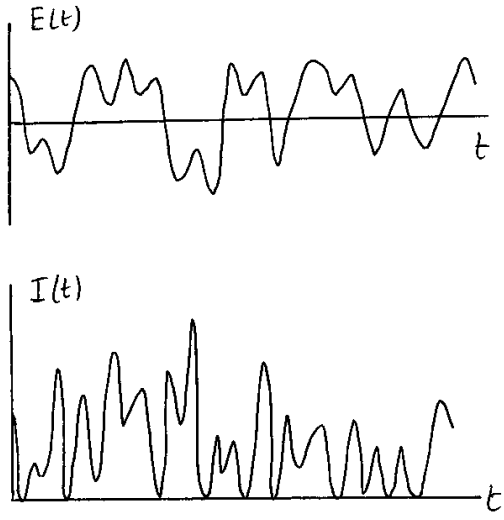

Figure 3.2: Typical variations of the electric field and of the intensity of a chaotic light source as functions of time. As electric field fluctuates around zero, the intensity vanishes very often.

Figure 3.2 shows the typical variations of the electric field of a chaotic source, and those of its intensity. Note that the intensity vanishes very often, because the field itself fluctuates around 0 (0 is the most likely value of the intensity), so that such a source must present very strong intensity fluctuations, however intense the source is. These intensity fluctuations can be characterized by another, second-order correlation function, or intensity correlation function (note the different normalizations in the first-order and second-order correlation functions!):

$$g^{(2)}(\tau) = \frac{\langle I(t+\tau)I(t)\rangle}{\langle I(t)\rangle^2} \quad .$$

With the expression of the field, expanding the product of four fields in the correlation, and taking the random phase into account, we can obtain the following relation (see Ex. 3.1), valid for a field resulting from a very large number of independent sources:

$$g^{(2)}(\tau) = 1 + \left|g^{(1)}(\tau)\right|^2 \quad .$$

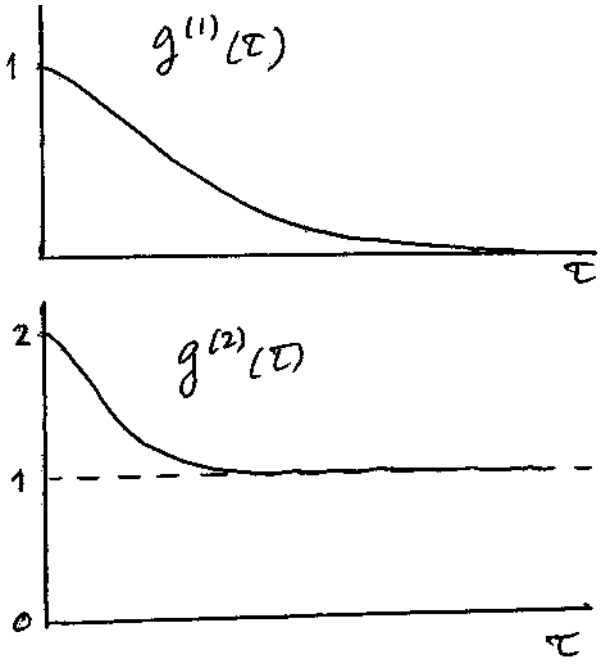

Figure 3.3: Variations of the first-order correlation function (of the field), and of the second-order correlation function (of the intensity), as functions of time for thermal or chaotic light. The Fourier transform of the first-order function is the intensity spectrum. Note the faster decay of the correlation function and the limit 1 for large times.

For thermal light, the intensity correlation function starts from 2 for short times and tends to 1 for long times (see Fig. 3.3). This spectrum of fluctuations does not scale as number fluctuations of independent particles: it could not be understood if photons

were independent grains emitted at random times. It arises from interference and is a consequence of the wave nature of light.

ii) coherent light:

A good example of a coherent light source is a well-stabilized cw laser. The classical coherent wave has constant amplitude, well-defined frequency and phase, and no fluctuations.

In the quantum representation of light, according to the correspondence principle, this coherent wave is just the limit of a packet of quantum states. The associated states are called coherent states. They are coherent superpositions of number states (or Fock states), i.e. states with well-defined numbers of photons. Coherent states are obtained by applying a translation operator to the vacuum state (i.e. no photon present in the mode), which leads to a minimal wavepacket oscillating in the harmonic potential without deformation. For a real parameter ξ (these relations can be generalized for a complex parameter ξ, representing the complex amplitude of the field), we have:

$|\xi\rangle = e^{S}|0\rangle$, with $S = \xi\left(a - a^{+}\right)$ and a translation operator $e^{S} = e^{-\xi a^{+}} e^{\xi a} e^{-\xi^{2}/2}$ leading to:

$$|\xi\rangle = e^{-\xi^{2}/2} \sum_{n} \frac{\xi^{n}}{\sqrt{n!}} |n\rangle$$

$|n\rangle$ being the Fock state with n photons in the mode of interest. The average number of photons in the coherent state is:

$\langle n\rangle = |\xi|^{2}$, and the distribution of photons is a Poisson distribution (represented in Fig.3.4):

$$p(m) = \frac{\langle n\rangle^{m}}{m!} e^{-\langle n\rangle} \quad .$$

From the above relations, we can easily check that $\langle n^{2}\rangle = |\xi|^{4} + |\xi|^{2} = \langle n\rangle^{2} + \langle n\rangle$.

The squared standard deviation of this distribution is:

$$\Delta n^{2} = \langle n^{2}\rangle - \langle n\rangle^{2} = \langle n\rangle \quad .$$

The fluctuations in the number of photons can be measured as fluctuations in the detection rate of an ideal photodetector. They give no correlation since, for a coherent

source with a constant intensity, the detection of one photon does not tell us anything about the probability to detect another photon at a later time. These fluctuations are therefore not "classical": they cannot be represented as a classical function of time $I(t)$. They are intrinsic to the nature of light and to the photodetection process, and are called "photon noise" or "shot noise". They give rise to the smallest possible intensity (or amplitude) noise in a "natural" (i.e. unsqueezed) coherent beam of light.

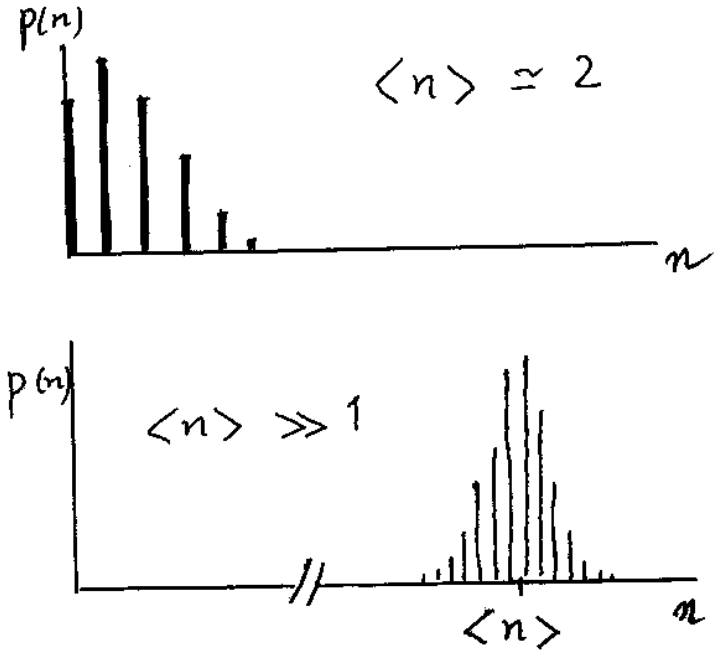

Figure 3.4: examples of the distribution of the number of photons in coherent states, with a small number of photons (top), or of a quasi-classical state with a large number of photons (bottom). In the limit of large numbers, the second distribution resembles a Gaussian.

iii) squeezed light:

In usual states of light (natural light), fluctuations are evenly distributed on two conjugated variables. For example, in a coherent state, both the electric and magnetic fields are subject to photon noise, or both the phase and the number of photons are subject to photon noise.

For some applications, it is interesting to reduce the noise on one of the conjugated variables, at the expense of more noise on the other one, according to Heisenberg's relations. Such a state of light is called squeezed light, and can be obtained from coherent light by a variety of nonlinear processes (linear processes conserve noise properties, and therefore cannot squeeze light). Figure 3.5 shows an example of waves squeezed in amplitude or in phase. Single nano-objects offer original ways to generate squeezed light.

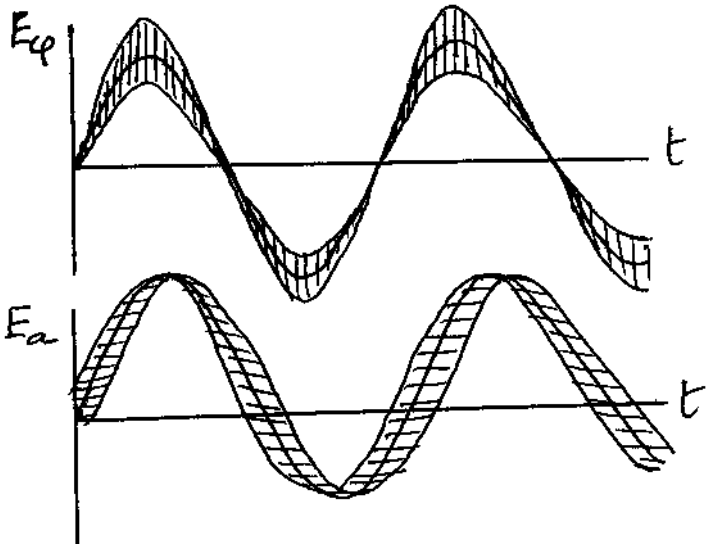

Figure 3.5: Schematic representation of the fluctuations of the field in the case of phase-compressed (top) and amplitude-compressed (bottom) light. Note the complementarity of noise on the conjugated variables phase and amplitude (or number of photons).

3.4.2 Methods

3.4.2.1. field correlation:

Classical spectroscopy provides the spectrum of the emitted light as a function of frequency, by means of filters (multiple-wave interferometers, monochromators) or dispersing devices (spectrographs).

Fourier-transform spectroscopy, i.e. two-wave interferometry, directly provides the auto-correlation function of the field $g^{(1)}(\tau)$, τ being the delay introduced by the interferometer between the two paths. The interferogram provides:

$$\left\langle \left| E(t) + E(t+\tau) \right|^2 \right\rangle \quad \propto \quad 2\left\{ 1 + \mathrm{Re}\left[g^{(1)}(\tau) \right] \right\},$$

which is related to the spectrum by a Fourier transformation.

3.4.2.2 intensity correlation:

i) direct correlation at long times: The second-order correlation function $g^{(2)}(\tau)$ would be obtained directly from a detector output if the detector was ideal. For times longer than microseconds, most detectors are good enough to enable either a direct electronic (hardware) accumulation of delays between all pairs of photons, or a software computation of $g^{(2)}(\tau)$ (see Fig. 3.6), as an integral of the product of $I(t)$

by a time-delayed copy of itself $I(t+\tau)$. It is important to realize that, for modern photon counting detectors, the intensity function reduces to a stream of δ-function-like detection events. The auto-correlation function $g^{(2)}(\tau)$ can then simply be evaluated as the histogram of pairs of photons separated by time-delay τ, created after some long accumulation time (see Ex. 3.2).

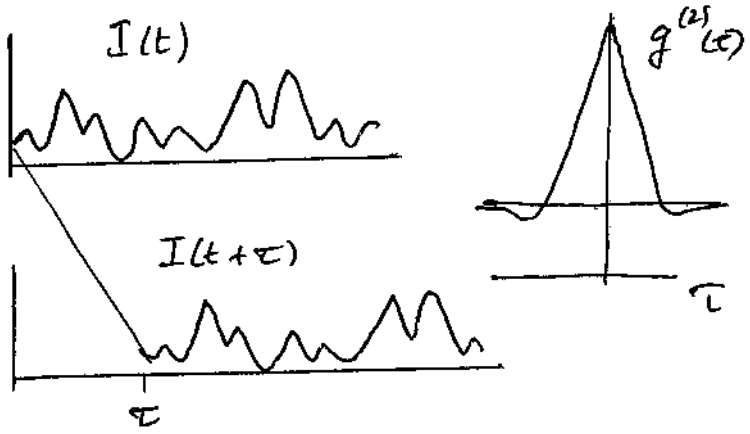

Figure 3.6: Correlation of an optical signal: the intensity is delayed by τ, multiplied by itself, and the integral of the product is plotted as a function of delay.

The correlation method provides access to slow fluctuations, which is very useful to study diffusion, fluctuations, slow chemical kinetics, etc., via such optical signals as light scattering, fluorescence, two-photon excited fluorescence, CARS, or other optical signals. Because slow processes can be spread over many orders of magnitude of time, it is convenient to plot the correlation function on a *logarithmic scale of time*, offering at a glance the main timescales of the fluctuations, and avoiding the sometimes lengthy search for the relevant timescale. To observe strong correlation in such experiments, it is important to collect light only from one 'coherence volume' (otherwise the contrast is severely reduced). This is usually achieved by a confocal arrangement, where a pinhole in the image plane restricts the detection volume contributing to the signal.

When the signal is a superposition of intensities of several single molecules or nano-objects, which is the case of fluorescence, the contrast of the correlation will decrease as the reciprocal of the number of independent emitters contributing to the detected signal.

Similarly, a constant or uncorrelated background *B* will reduce the contrast of the measured correlation $\tilde{g}^{(2)}(\tau)$ according to:

$$\tilde{g}^{(2)}(\tau)-1 \quad = \quad \frac{\langle (B+I(t))(B+I(t+\tau)\rangle}{(B+I)^2}-1 \quad = \quad \left(1+\frac{B}{I}\right)^{-2}\left(g^{(2)}(\tau)-1\right)$$

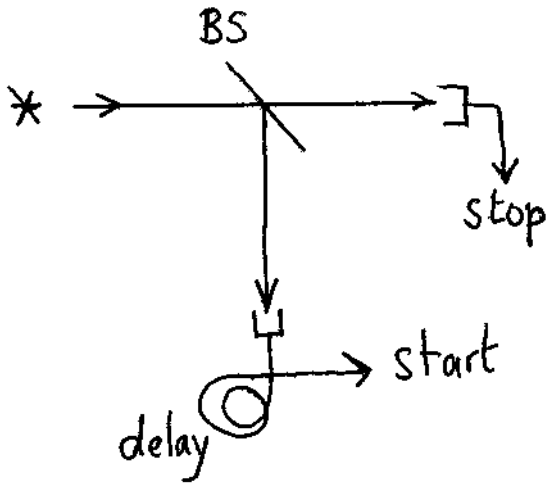

Figure 3.7: A start-stop experiment, where the histogram of delays between the start and stop pulses is measured. Thanks to a delay of the start signal, "negative" times can also be investigated.

ii) start-stop at short times: For times shorter than microseconds, real detectors suffer from dead time and afterpulsing. Dead time is the time following each detection event, during which a detector is blind to other photons. Afterpulses are spurious events triggered later than the initial detection by stray ions in a photomultiplier or by stray charge carriers in an avalanche photodiode. To eliminate both these effects, Hanbury-Brown and Twiss proposed to use two detectors, to split the light beam to be analyzed, and to measure *coincidences* between detection events in the two arms (see Fig.3.7). The coincidence histogram provides a cross-correlation function, which is free from dead-time effects because the stop detector is not blinded by detection in the start detector, and free from afterpulsing effects for the same reason. For practical electronic reasons, it is much simpler to do a start-stop experiment, i.e. to record only the first photon arriving in the stop arm after one photon has been detected in the start arm. The histogram of time delays between start and stop events gives the distribution function of consecutive pairs, $C(\tau)$. We define $C(\tau)$ as the probability of observing the *next* photon at time τ, knowing that a first photon has been observed at time 0. Similarly, we define $P(\tau)$ as the probability of observing *any* other photon at time τ, knowing that the first photon was observed at time 0. $P(\tau)$ is related to the correlation function by:

$P(\tau) = \langle I(t)\rangle\, g^{(2)}(\tau)$.

For steady-state Markovian emission processes, i.e. if the system is reset to the same initial conditions after each detection event, $C(\tau)$ can be easily related to $P(\tau)$ by renewal theory. The probability to detect any photon after some delay is the probability that this photon is the next one, plus the probability that it is the second one, plus etc.:

$$P(\tau) = C(\tau) + \int_0^\tau C(\tau - t_1) C(t_1)\, dt_1 + \int_0^\tau dt_1\, C(\tau - t_1) \int_0^{t_1} dt_2\, C(\tau - t_2)\, C(t_2) + \ldots$$

The Laplace transforms of these distributions are therefore related by:

$$\tilde{P}(s) = \tilde{C}(s) + \tilde{C}(s)^2 + \tilde{C}(s)^3 + \ldots = \frac{\tilde{C}(s)}{1 - \tilde{C}(s)} \quad .$$

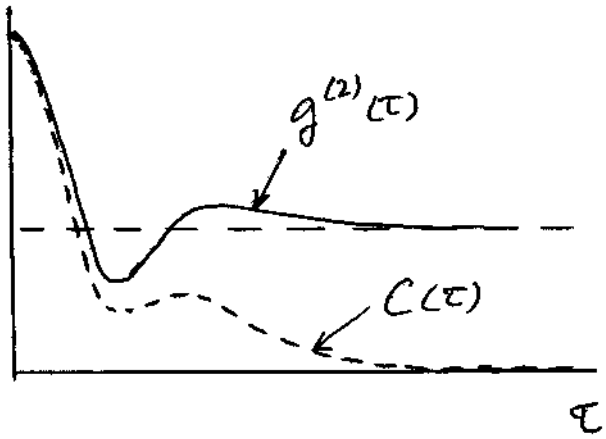

Figure 3.8: Example of compared variations of the correlation function (distribution of all photon pairs) and of the distribution of consecutive pairs C(τ), with suitable normalization. Note the exponential decrease of the latter function for long times.

The main difference between these two distribution functions appears for long times (see Fig.3.8). Then, $C(\tau)$ decreases exponentially as $\exp(-\langle I \rangle \tau)$, i.e. as the probability not to observe any photon during time τ, whereas $P(\tau)$ tends to a constant, $\langle I \rangle$. For this reason, the start-stop technique cannot be used to investigate long correlation times.

The correlation function of a classical function of time must have an absolute maximum for time 0. This follows from the concavity of a quadratic function:

$\langle I(t) \rangle^2 \leq \langle I^2(t) \rangle$.

Therefore, photons from a classical source tend to arrive in bunches or packets. This effect is often called photon bunching.

On short times, however, a single molecule will emit only one photon at a time, so that the correlation function is nil for time 0 (see below). When the correlation function is such that:

$g^{(2)}(0) < 1$

one speaks of photon antibunching. This is a non-classical effect. When it occurs, it shows strikingly that such "non-classical" light cannot be described by a classical function of time.

3.4.2.3 other analysis methods:

The statistics of the photon stream may be analysed in other ways. For example, one may plot a histogram of the signal intensities in a given short time interval. This shows whether the signal has preferred values (peaks in the distribution), or deviates from the Poisson distribution (Fig.3.4) expected for a constant intensity. This technique is sometimes called burst size analysis, in the case of fluid solutions. A related way to characterize instantaneous intensity fluctuations is to plot the histogram $C(\tau)$ of delay times between consecutive photons.

In many cases, single nano-objects show distinct on- and off-times, a phenomenon called *blinking*. Defining an intensity threshold at a given time resolution, on can plot histograms of the durations of on- and off-times, which also give valuable information about the systems fluctuations. Change point algorithms are programs searching for the most likely points of intensity changes in an experimental time trace, obviating part of the arbitrariness in choosing thresholds and bin sizes.

3.4.3. Pulsed sources

It is a special feature of single objects that time-resolved information can be obtained with cw excitation, whereas it is usually obtained with pulsed excitation on ensembles. Although we assumed so far that the excitation of the emitter was steady-state or cw, it is also interesting to apply pulsed techniques to single emitters.

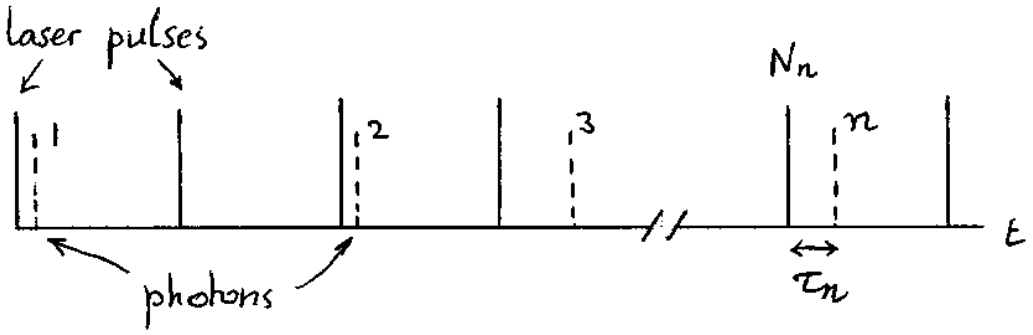

Figure 3.9: Recording of two times for each detected photon. Macroscopic time given by the date of the laser pulse, and nano- or micro-scopic one by the delay with respect to the excitation laser pulse.

3.4.3.1 Time-Correlated Single-Photon Counting (TCSPC): with this method, one builds a histogram of the arrival times of the single photon recorded after each excitation pulse. When TCSPC is applied to a large ensemble, one has to take care that much less than one photon on average be detected after each laser pulse. Otherwise, pile-up occurs, i.e. the histogram is biased towards short times because the first detected photon prevents the acquisition of later ones. In the case of a single emitter, however, no pile-up may occur: only one photon can be emitted after each excitation pulse, at least if background is negligible. A TCSPC histogram directly shows the (often single-exponential) decay of the excited state population created by the pulse, and gives the fluorescence lifetime of the object.

3.4.3.2 Recording of the full time information: The laser pulses are considered as a clock, giving the “macroscopic” time at which the system is excited. The delay between laser pulse and fluorescence photon gives the “nanoscopic” time, characteristic of the fluorescence lifetime (see Fig. 3.9). On a long acquisition series of photons from single objects, it is often useful to record both times. With 100 to 1000 events, the “instantaneous” fluorescence lifetime can be correctly estimated, and the variations of this quantity with macroscopic time can be investigated. Fluctuations of the fluorescence lifetime can arise from conformational changes, photochemical processes, fluorescence quenching, etc. Commercial dedicated electronic boards can sort and store long series of macroscopic and microscopic times corresponding to each detected photon.

Exercise 3.1: For a large number of independent sources the intensity correlation function $g^{(2)}(\tau)$ *can be written simply with the first-order field correlation function* $g^{(1)}(\tau)$ *as:* $g^{(2)}(\tau) = 1 + \left[g^{(1)}(\tau) \right]^2$.

Writing the total field as a sum of many field components with random phases, prove this relation between the two functions.

Hint: notice that in the product of four sums of fields appearing in the second-order correlation function, there are two ways of eliminating the random phases, therefore two types of terms that will survive the averaging.

Exercise 3.2: Writing the intensity as a sequence of delta functions at photon detection times t_i *:*

$$I(t) = \sum_i \delta(t - t_i),$$

prove that, in the limit of infinite accumulation time, the second-order correlation function is a histogram of all photon pairs separated by time $\tau = t_i - t_j$.

Exercise 3.3: Prove the following relation between theoretical correlation function $g^{(2)}(\tau)$ *and the one measured in the presence of background* $\tilde{g}^{(2)}(\tau)$*:*

$$\tilde{g}^{(2)}(\tau) - 1 \quad = \quad \frac{\left\langle [B + I(t)][B + I(t+\tau)] \right\rangle}{(B+I)^2} - 1 \quad = \quad \left(1 + \frac{B}{I}\right)^{-2} \left(g^{(2)}(\tau) - 1 \right)$$

Exercise 3.4: The probability of a time delay τ *between two consecutive photons detected from a coherent beam is* $p(\tau) = \gamma \exp[-\gamma\tau]$ *(Poisson statistics). Prove that the probability of observing n photons during time* T *is* $q_n(T) = \frac{(\gamma T)^n}{n!} \exp(-\gamma T)$.

Hint: find first the probability $q_0(T)$ *of observing no photon during time* T *. Then deduce the probability* $q_1(T)$ *of observing one photon during that time, and by recursion deduce the above result.*